Supplementary Information for:

Crystal Structure of Cysteamine Dioxygenase Reveals the Origin of the Large Substrate Scope of this Vital Mammalian Enzyme

Rebeca L. Fernandez,[1] Laura D. Elmendorf,[1] Robert W. Smith,[2] Craig A. Bingman,[2] Brian G. Fox,[2] and Thomas C. Brunold[1]*

[1]Department of Chemistry, University of Wisconsin-Madison, Madison, Wisconsin 53706, United States
[2]Department of Biochemistry, University of Wisconsin-Madison, Madison, Wisconsin 53706, United States

* Corresponding author: brunold@chem.wisc.edu

Table S1. Data collection and refinement statistics

Wavelength (Å)	1.127	
Space group	P 21 21 21	
Unit cell	a=54.296 Å, b=139.525 Å, c=142.007 Å, α=β=γ=90°	
Data collection statistics		
	overall	last shell
Resolution range (Å)	39.17 – 1.89	1.958 – 1.89
Total reflections	1144403	108025
Unique reflections	86883	4059
Multiplicity	13.2	12.6
Completeness (%)	87.21	47.39
Mean I/σ(I)	12.34	0.99
Wilson B-factor	34.34	
R-merge	0.1844	1.657
R-meas	0.1919	1.726
R-pim	0.05248	0.4784
CC(1/2)	0.994	0.474
CC*	0.998	0.802
Refinement statistics		
Reflections used in refinement	76076	4059
Reflections used for R-free	2519	161
R-work	0.1911	0.2749
R-free	0.2275	0.3125
CC(work)	0.954	0.753
CC(free)	0.945	0.789
Number of non-hydrogen atoms	8168	
macromolecules	7597	
ligands	10	
solvent	561	
Protein residues	965	
RMS bonds (Å)	0.01	
RMS angles (°)	0.88	
Ramachandran favored (%)	98.09	
Ramachandran allowed (%)	1.49	
Ramachandran outliers (%)	0.42	
Rotamer outliers (%)	0.36	
Clashscore	1.79	
Average B-factor (Å^2)	46.47	
Macromolecules (Å^2)	46.74	
Ligands (Å^2)	42.78	
Solvent (Å^2)	42.91	
Number of TLS groups	16	

Table S2. Results from a SuperPose analysis for the four different ADO monomers in the unit cell. http://superpose.wishartlab.com

Maiti R, Van Domselaar GH, Zhang H, Wishart DS. SuperPose: a simple server for sophisticated structural superposition. Nucleic Acids Res. 2004 Jul 1;32(Web Server issue):W590-4. doi: 10.1093/nar/gkh477. PMID: 15215457; PMCID: PMC441615.

Chains A and B

Global RMSD

	Alpha Carbons	Back Bone	Heavy	All
RMSD	1.30	1.31	1.72	1.90
Atoms	236	944	1859	3697

Structure	Residues
PDBA chain 'A'	7-22, 31-217, 224-256
PDBB chain 'B'	7-22, 31-217, 224-256

Chains A and C

Global RMSD

	Alpha Carbons	Back Bone	Heavy	All
RMSD	1.19	1.18	1.43	1.60
Atoms	236	944	1852	3679

Structure	Residues
PDBA chain 'A'	7-21, 22-22, 31-217, 224-256
PDBB chain 'C'	7-21, 30-30, 31-217, 224-256

Chains A and D

Global RMSD

	Alpha Carbons	Back Bone	Heavy	All
RMSD	1.18	1.21	1.61	1.80
Atoms	236	944	1859	3698

Structure	Residues
PDBA chain 'A'	7-22, 31-217, 224-256
PDBB chain 'D'	7-22, 31-217, 224-256

Chains B and C

Global RMSD

	Alpha Carbons	Back Bone	Heavy	All
RMSD	0.69	0.70	1.08	1.33
Atoms	238	952	1862	3698

Structure	Residues
PDBA chain 'B'	7-21, 30-217, 222-256
PDBB chain 'C'	7-21, 30-217, 222-256

Chains B and D

Global RMSD

	Alpha Carbons	Back Bone	Heavy	All
RMSD	1.70	1.65	1.87	2.04
Atoms	243	972	1902	3780

Structure	Residues
PDBA chain 'B'	7-22, 30-256
PDBB chain 'D'	7-22, 30-256

Chains C and D

Global RMSD

	Alpha Carbons	Back Bone	Heavy	All
RMSD	1.44	1.44	1.63	1.82
Atoms	238	952	1862	3700

Structure	Residues
PDBA chain 'C'	7-21, 30-217, 222-256
PDBB chain 'D'	7-21, 30-217, 222-256

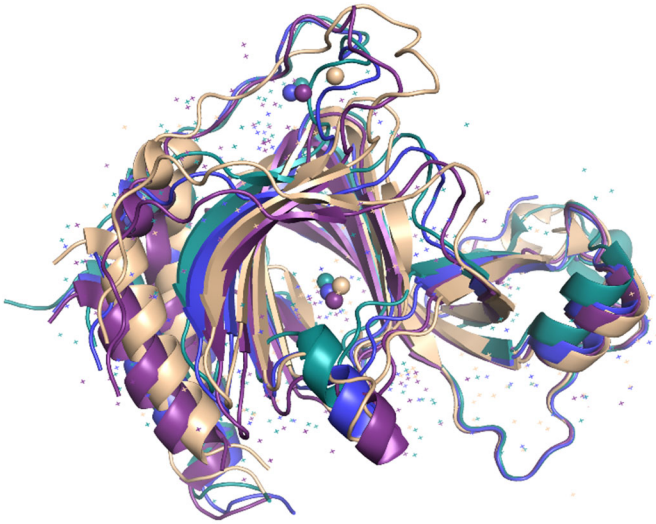

Figure S1. Overlay of the four independent ADO monomers in the unit cell. Chain A is shown in blue, chain B yellow, chain C green, and chain D purple. The spheres in the center of the protein are the Fe atoms and the ones near the periphery are either Cl or Mg atoms.

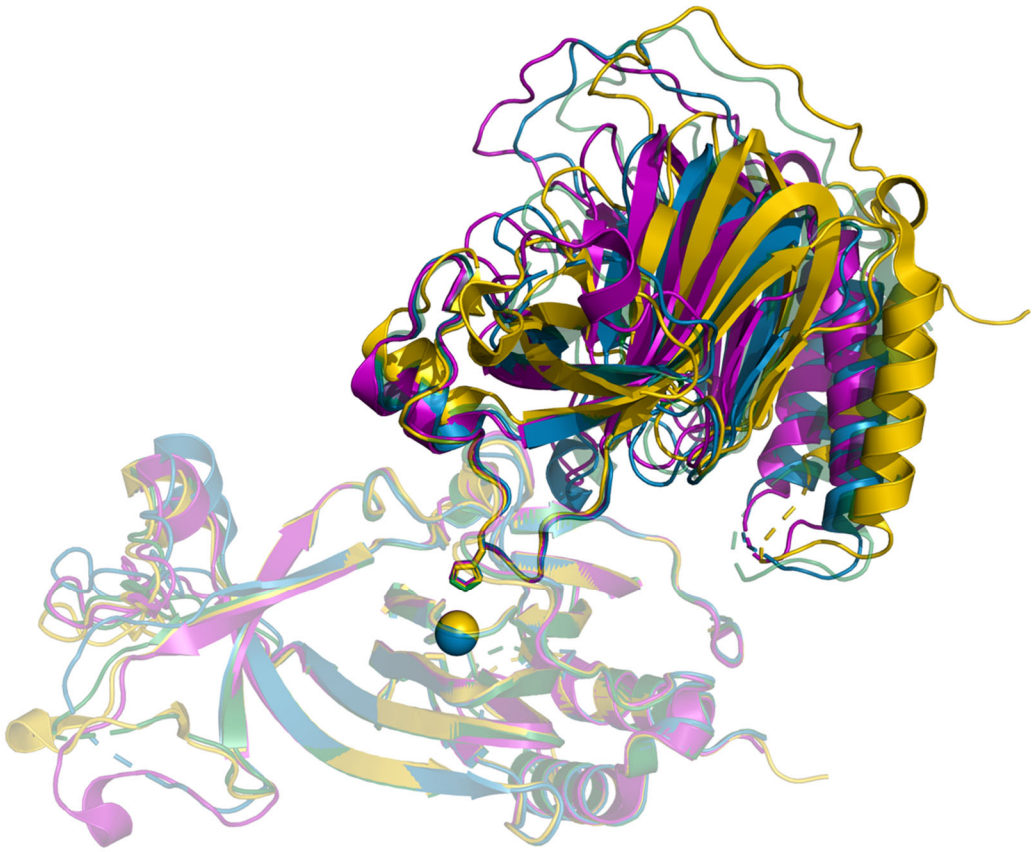

Figure S2. His130 from a neighboring molecule intrudes into the active site in each of the four crystallographically unique copies of *Mm*ADO. The four chains were superposed along with their interacting partners in the crystal. The superposed molecules are transparent, their interacting molecules are not, and His130 is rendered as sticks.

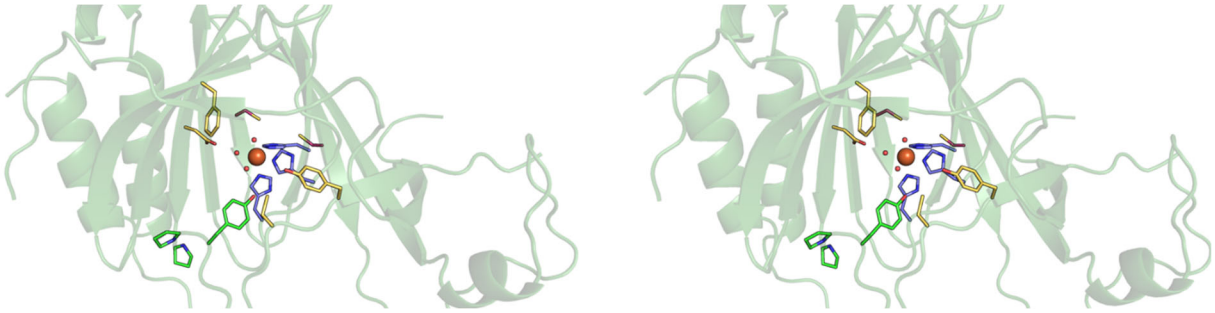

Figure S3. Stereo view of the active site region of *Mm*ADO.

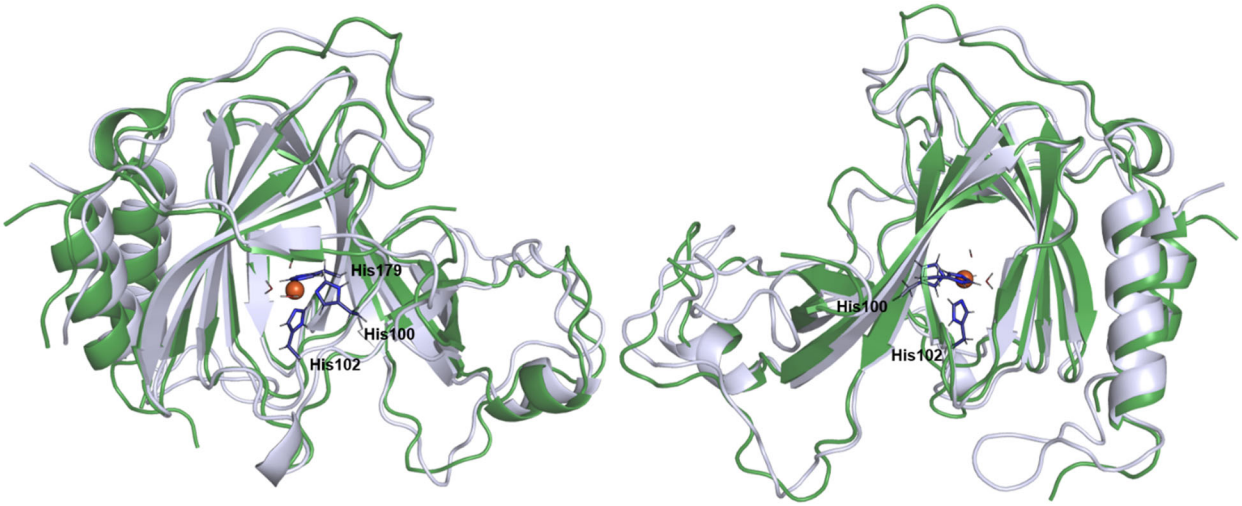

Figure S4. Comparison of the ADO X-ray crystal structure with a QM/MM optimized structure of ADO. The X-ray structure is shown in green and the QM/MM optimized model in gray.

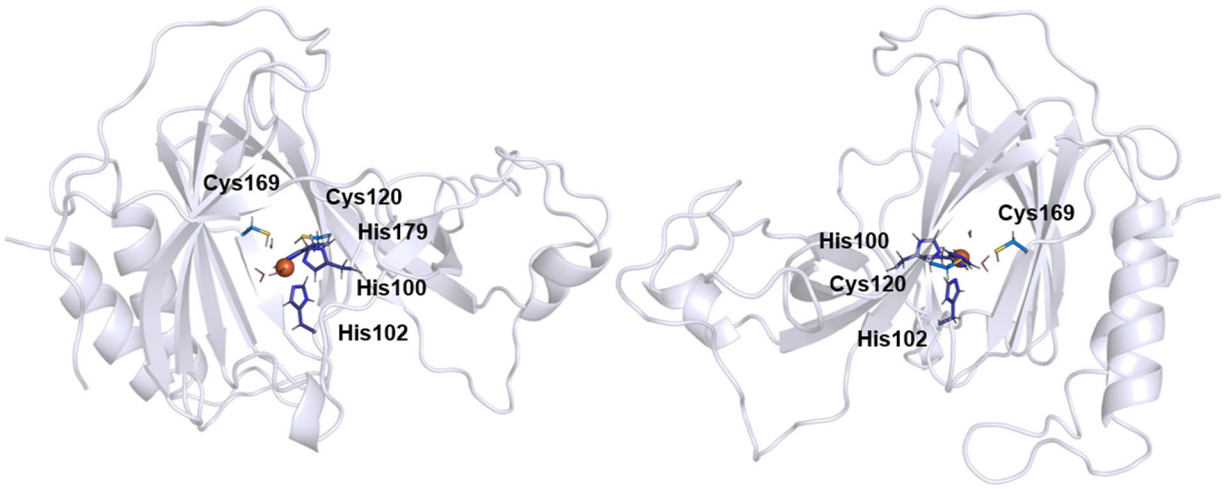

Figure S5. Front and back of the QM/MM optimized structure of ADO.

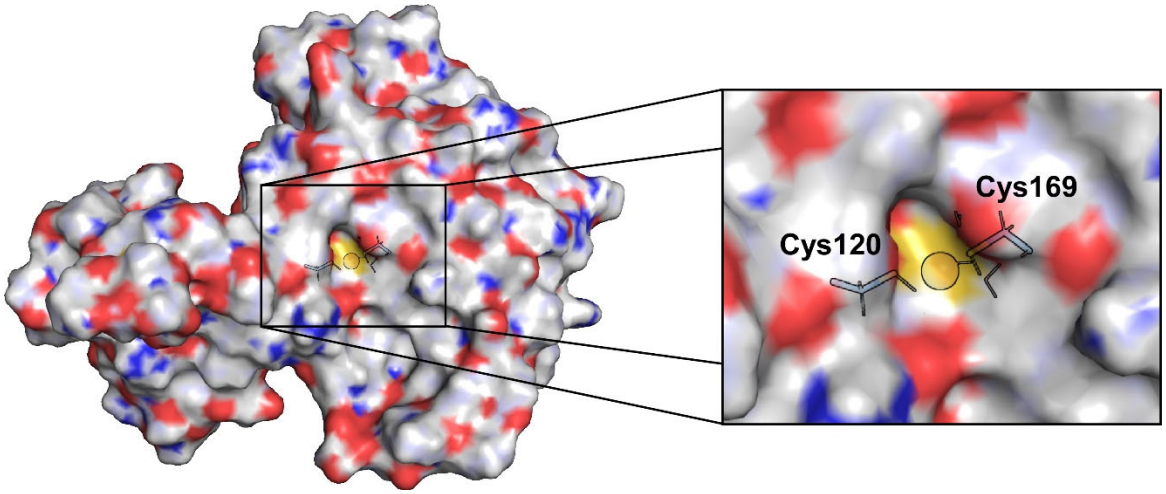

Figure S6. Surface representation of the backside of QM/MM optimized structure of ADO highlighting the co-substrate tunnel. The RBG coloring is as follows: Fe, orange; carbon, green; hydrogen white, oxygen, red; nitrogen, blue; and sulfur, yellow.

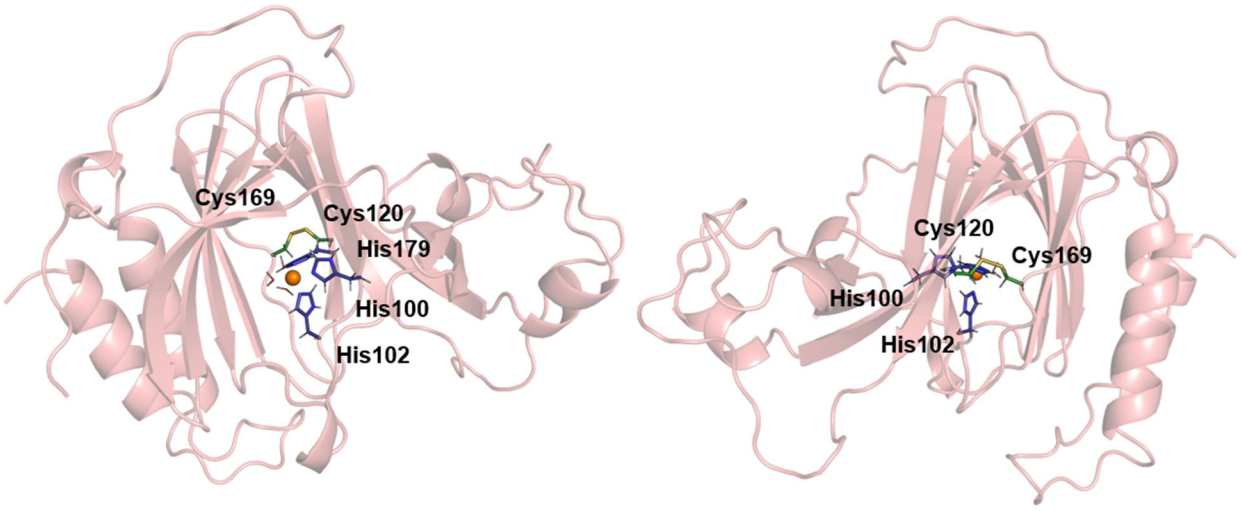

Figure S7. Front and back of the QM/MM optimized structure of a putative form of oxidized ADO. This structure has a disulfide bond between Cys120 and Cys169 (disulfide bond in yellow).

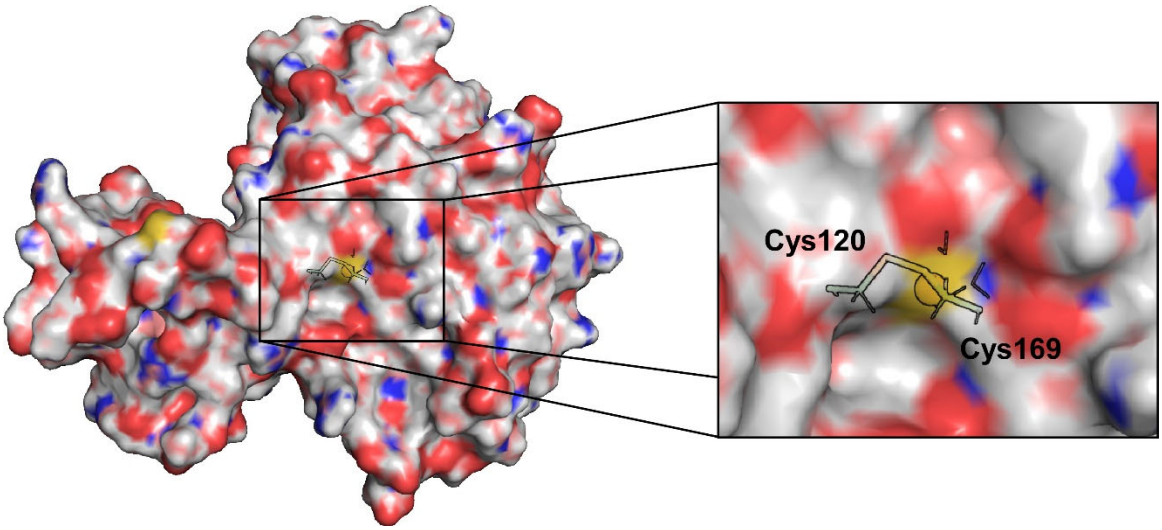

Figure S8. Surface representation of the backside of QM/MM optimized structure of oxidized ADO. A disulfide bond between Cys120 and Cys169 closes the back co-substrate tunnel. The RBG coloring is as follows: Fe, orange; carbon, green; hydrogen white, oxygen, red; nitrogen, blue; and sulfur, yellow.

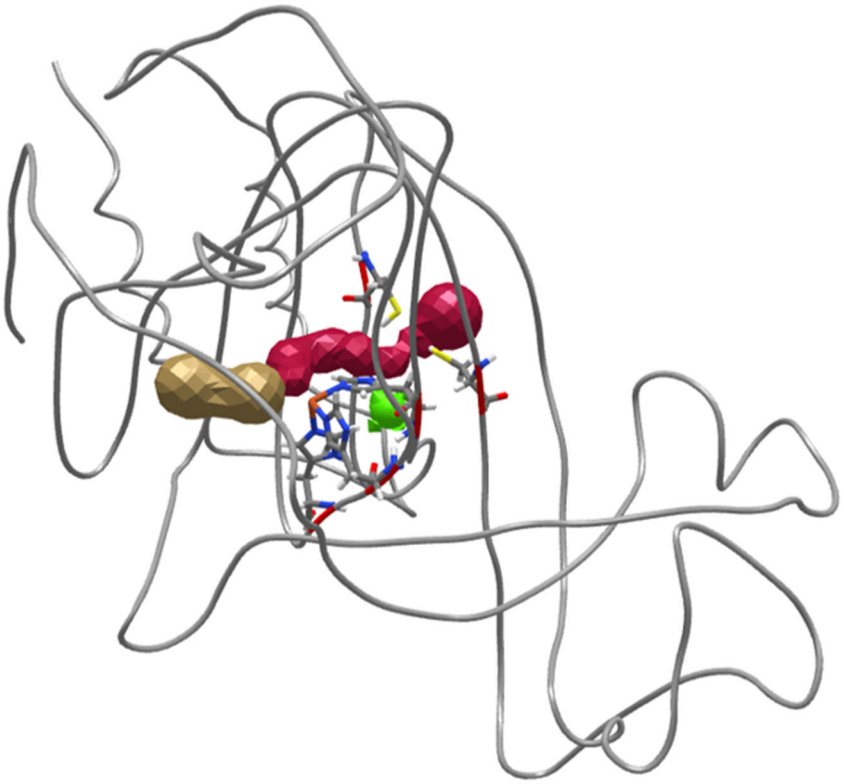

Figure S9. Tunnels calculated by MOLE2.5 into the active site of the QM/MM optimized model of peptide-bound ADO. To generate these tunnels the following parameters were used: internal threshold of 0.9 Å, bottleneck radius of 0.49 Å, and a cutoff ratio of 0.5.